Gapless Quantum Spin Liquid in the Triangular System $Sr_3CuSb_2O_9$

S. Kundu,[1,*] Aga Shahee,[1] Atasi Chakraborty,[2] K. M. Ranjith,[3] B. Koo,[3] Jörg Sichelschmidt,[3] Mark T. F. Telling,[4] P. K. Biswas,[4] M. Baenitz,[3] I. Dasgupta,[2] Sumiran Pujari,[1] and A. V. Mahajan[1,†]

[1]*Department of Physics, Indian Institute of Technology Bombay, Powai, Mumbai 400076, India*

[2]*School of Physical Sciences, Indian Association for the Cultivation of Science, Jadavpur, Kolkata 700032, India*

[3]*Max Planck Institute for Chemical Physics of Solids, 01187 Dresden, Germany*

[4]*ISIS Pulsed Neutron and Muon Source, STFC Rutherford Appleton Laboratory, Harwell Campus, Didcot, Oxfordshire OX110QX, United Kingdom*

(Received 13 August 2020; accepted 1 December 2020; published 28 December 2020)

We report gapless quantum spin liquid behavior in the layered triangular $Sr_3CuSb_2O_9$ system. X-ray diffraction shows superlattice reflections associated with atomic site ordering into triangular Cu planes well separated by Sb planes. Muon spin relaxation measurements show that the $S = \frac{1}{2}$ moments at the magnetically active Cu sites remain dynamic down to 65 mK in spite of a large antiferromagnetic exchange scale evidenced by a large Curie-Weiss temperature $\theta_{CW} \simeq -143$ K as extracted from the bulk susceptibility. Specific heat measurements also show no sign of long-range order down to 0.35 K. The magnetic specific heat (C_m) below 5 K reveals a $C_m = \gamma T + \alpha T^2$ behavior. The significant T^2 contribution to the magnetic specific heat invites a phenomenology in terms of the so-called Dirac spinon excitations with a linear dispersion. From the low-T specific heat data, we estimate the dominant exchange scale to be ~36 K using a Dirac spin liquid ansatz which is not far from the values inferred from microscopic density functional theory calculations (~45 K) as well as high-temperature susceptibility analysis (~70 K). The linear specific heat coefficient is about 18 $\mathrm{mJ/mol\,K^2}$ which is somewhat larger than for typical Fermi liquids.

DOI: 10.1103/PhysRevLett.125.267202

Introduction.—The search for novel spin liquids has been driving the community of quantum magnetism ever since the proposal of Fazekas and Anderson [1]. It is now theorized that spin liquids come in various flavors, may have gapped or gapless excitations, may be topological or not [2]. Frustration disfavors magnetic order and is thus generically sought as a route to realizing spin liquids. Geometric frustration from the lattice composed of triangular motifs forms a key class in this search going back to the Fazekas-Anderson work for the triangular lattice [1]. While the $S = \frac{1}{2}$ uniform triangular lattice (with nearest-neighbor Heisenberg exchange J_1) has 120° long-range order [3–5] also supported by theory [6–10], the presence of further neighbor exchanges has been argued to enhance frustration and induce spin liquid behavior [11–13]. One candidate state for such a spin liquid has linearly dispersing low-energy excitations [14] and has been dubbed as a Dirac quantum spin liquid (QSL). They lead to a T^2 variation of the heat capacity in zero magnetic field, and an additional linear-in-T variation in the presence of a magnetic field. For $S = \frac{1}{2}$ triangular lattices, previously reported spin liquids [15–21] have not shown a T^2 behavior in the specific heat. Here, we report on the finding of such a candidate Dirac QSL in the $Sr_3CuSb_2O_9$ (SCSO) triangular lattice system.

Taking inspiration from the triple perovskite $Ba_3CuSb_2O_9$ (of the form $A_3B_3X_9$) with a hexagonal lattice which has been inferred to be a $S = \frac{1}{2}$ QSL [22,23], we considered the possibility of replacing the Ba^{2+} by the smaller Sr^{2+} ion resulting in chemical pressure and concomitant effects on the crystal structure and the magnetic ground state. Reference [24] has reported on the dielectric properties of $Sr_3CuNb_2O_9$ while SCSO is largely unexplored. These triple perovskites crystallize in the tetragonal crystal system which is different from that of $Ba_3CuSb_2O_9$. Significantly different ionic sizes and charges of Sb^{5+} (0.60 Å) and Nb^{5+} (0.64 Å) compared to Cu^{2+} (0.73 Å) should favor atomic site ordering at the B sites. This has also been seen in homologous compounds $Sr_3CaIr_2O_9$ [25] and $Sr_3CaRu_2O_9$ [26]). With 1:2 ordering at the B site, the (111) planes (pertinent to the pseudocubic lattice) will have successive Cu planes with an edge-shared triangular geometry separated by two Sb/Nb planes (see Fig. 1 for a schematic). X-ray diffraction indeed shows superlattice peaks supporting this site ordering in SCSO.

Our experiments on SCSO have shown the following salient results: (1) The bulk susceptibility of SCSO shows no sign of long-range order (LRO) down to 1.8 K. It shows Curie-Weiss behavior with a Curie-Weiss temperature $\theta_{CW} \simeq -143$ K. There is no bifurcation in the zero-field

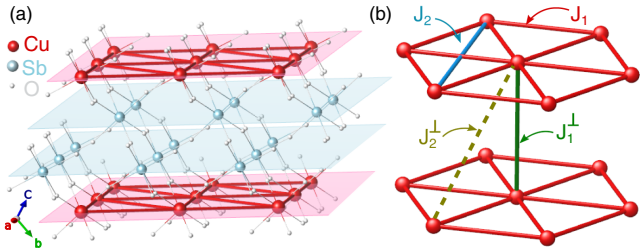

FIG. 1. (a) A schematic of the SCSO crystal structure is shown highlighting the individual planes of Cu (red) and Sb (blue) atoms. The Sr atoms are omitted for visual clarity. (b) The paths corresponding to different exchange couplings.

cooled (ZFC) and field cooled (FC) magnetization in low field either. (2) Zero-field muon spin relaxation (ZF-μSR) data reconfirm the absence of any magnetic ordering down to 65 mK. Longitudinal-field μSR (LF-μSR) data show that the moments remain dynamic down to very low temperatures. (3) Magnetic heat capacity data are also devoid of any indications of a phase transition down to 0.35 K. A $\gamma T + \alpha T^2$ form is seen in the low-T behavior.

An unequivocal presence of a T^2 contribution in the magnetic specific heat, in the absence of any evidence of magnetic order, naturally suggests a phenomenology in terms of a Dirac QSL. Density functional theory (DFT) calculations for the B-site ordered structure also support a model of SCSO as a triangular lattice quantum antiferromagnet with small further-neighbor frustrating antiferromagnetic exchanges [in the (111) planes pertinent to the pseudocubic cell] for which a Dirac QSL has been predicted [11–13].

Results and discussion.—The Rietveld refinement of XRD data on our polycrystalline SCSO sample by FullProf suite software [27] is shown in Fig. 2. Fitting with a body-centered tetragonal structure with space group $I4/mcm$ (140) [shown in Supplemental Material (SM) [28]] does not account for a few peaks at low angles (region shown in the inset of Fig. 2). 1:2 atomic site ordering refines the data well with a propagation vector $\vec{K} = (\frac{1}{3}, \frac{1}{3}, \frac{1}{3})$. The obtained lattice parameters are $a = b = 5.547$ Å, $c = 8.248$ Å.

Figure 3 shows the dc susceptibility, $\chi(T)\{= [M(T)/H]\}$ of SCSO in $H = 1$ kOe. No indications of long-range order are seen down to 2 K. We fit the data (in the high-temperature range of 150–300 K) to the theoretical triangular lattice antiferromagnet (TLAF) model for a 2D spin-1/2 system [33] using $\chi = \chi_0 + \chi_{\mathrm{TLAF}}$ as in Refs. [34,35]. Here, χ_0 is the temperature independent susceptibility (arising from core diamagnetism and a van Vleck contribution), $C = N_A g^2 \mu_B^2 / 4k_B$ is the Curie constant, and J_1 is the nearest neighbour exchange coupling [36]. Fixing $C = 0.375$ K cm^3/mol Cu for our $S = \frac{1}{2}$ system, this TLAF fit yields $\chi_0 = -2.10 \times 10^{-4}$ cm^3/mol Cu, and $|J_1/k_B| = 70$ K [37].

The inset of Fig. 3 shows the ZFC/FC susceptibility. No bifurcation is seen down to 2 K. AC susceptibility data (see SM [28]) show no anomaly either. This rules out the existence of spin-glass behavior in the system [38].

Additional evidence for the absence of static magnetism down to even lower temperatures (65 mK) was gathered from μSR experiments. The ZF muon asymmetry was measured as a function of T between 65 mK and 4 K. Strong relaxation of the muon is seen at the lowest temperature and we fit the time dependence of the asymmetry to $A(t) = A_0 G_{KT}(\Delta, t) e^{-\lambda(T)t} + A_{bg}$. Here, $G_{KT}(\Delta, t)$ is the static Kubo-Toyabe Gaussian function coming from relaxation due to the nuclear moments whereas the exponential decrease is from the relaxation due to electron moments. A_{bg} is the constant background signal (due to a small fraction of the muons missing the sample and hitting the sample holder and cryostat wall) and A_0 is the initial muon asymmetry. The muon asymmetry data at various T are shown in Fig. 4. The absence of

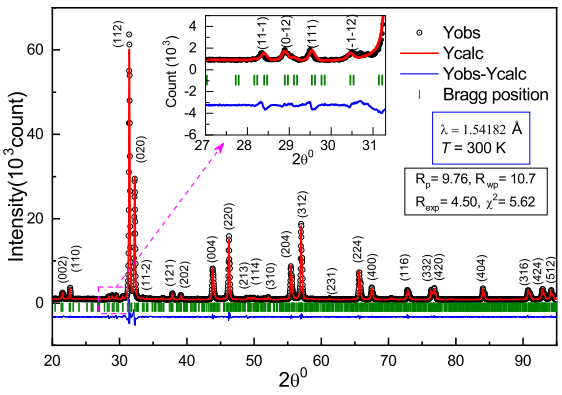

FIG. 2. Rietveld refinement of $Sr_3CuSb_2O_9$ is shown along with Bragg positions and corresponding Miller indices (hkl) with K modulation ($\frac{1}{3}$, $\frac{1}{3}$, $\frac{1}{3}$) (referred to a pseudocubic cell) to fit the superlattice peaks.

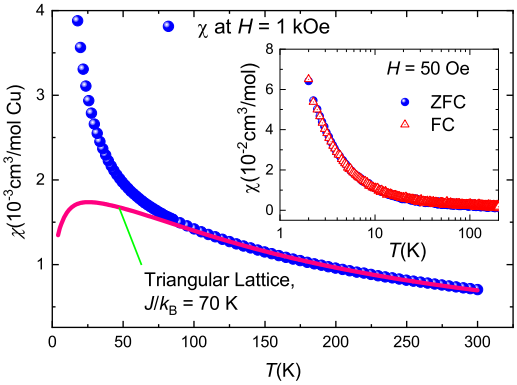

FIG. 3. The variation of $\chi(T)$ for SCSO in $H = 1$ kOe is shown in the main figure. The solid line is a theoretical TLAF fit for data in the range 150–300 K and then extrapolated down to 2 K. In the inset, no bifurcation is seen in the plot of $\chi(T)$ vs T between ZFC and FC data in $H = 50$ Oe.

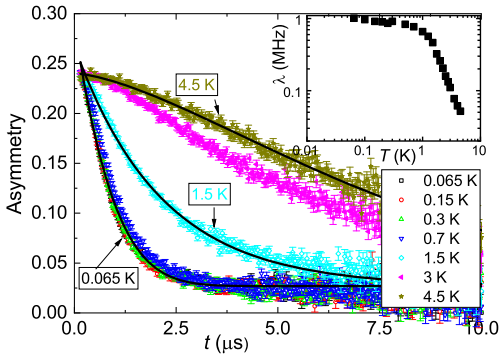

FIG. 4. The variation of the muon asymmetry with time is shown at various temperatures in zero field for $Sr_3CuSb_2O_9$. On fitting these data as described in the text, the muon relaxation rate was obtained and is shown in the inset.

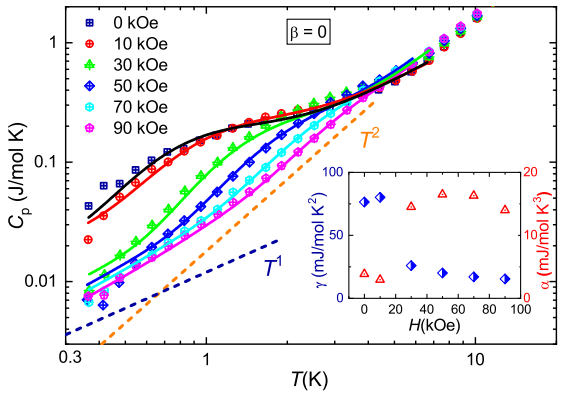

FIG. 5. The heat capacity of SCSO is plotted as a function of temperature in various fields. The solid lines are fits as explained in the text. Dashed lines represent power law variations T^1 and T^2. Inset: The variation of the coefficients of the linear (blue diamonds; left y-axis) and quadratic (red triangles; right y-axis) terms is shown as a function of H.

oscillations in the muon asymmetry data suggests the absence of any short or long-range magnetic ordering down to 65 mK. Further, the absence of the one-third tail suggests the dynamic nature of the electronic spins. The LF-μSR data will further validate the dynamic nature of the moments.

As seen in Fig. 4, the relaxation curves are essentially unchanged from 65 mK to about 1 K and at higher temperatures, the muon depolarization rate decreases. From the above analysis, the muon relaxation rate due to electron moments is obtained as shown in the inset of Fig. 4. It is seen that there is a gradually faster relaxation of muons with a lowering of temperature. However, there is no large increase or a critical divergence and the electron moments remain dynamic till the lowest temperatures.

We have also monitored muon relaxation in longitudinal fields and find that even in our highest field of 3200 Oe, residual relaxation is still present (see SM [28]). The field dependence is remarkably similar to that of $YbMgGaO_4$ [39] with a local moment fluctuation frequency of about 18 MHz and the presence of long-time spin correlations. The qualitative and quantitative outcomes of μSR on SCSO are typical of other QSL.

To further rule out LRO and to probe the nature of low-energy excitations, we measured the heat capacity of the sample $C_p(T)$ in different fields (0–90 kOe) in the T range (0.35–200) K. As shown in Fig. 5, a hump is seen in the heat capacity which moves to higher temperatures with increasing field, and can be ascribed to the Schottky anomaly commonly seen in many quantum magnets [22,40,41]. This arises from a small fraction of free spins (either of extrinsic origin or from edge spins of correlated regions). In the low-T regime, the scaling is observed to be close to T^2. This already hints at the presence of linearly dispersing excitations. We thus model the specific heat below 6 K as $C_p(T,H) = \gamma(H)T + \alpha(H)T^2 + fC_{\text{Schottky}}(T,H)$ motivated by a Dirac QSL phenomenology. C_{Schottky} is the standard Schottky contribution of a wo-level system (see SM [28]) with f being the fraction of free $S = \frac{1}{2}$ entities. Solid lines in Fig. 5 show fits to the as-measured C_p with the parameter values $\gamma_{\text{avg}} = 18\ \text{mJ/mol K}^2$, $\alpha_{\text{avg}} = 15\ \text{mJ/mol K}^3$, and $f = 2.5\%$. For γ and α, the quoted average is over the fits for $H \geq 30$ kOe. The Schottky fraction f was obtained from the fit for 90 kOe data and kept fixed for other fields. A βT^3 contribution from the lattice can also be included in the analysis, but it makes no essential difference to the fits. Fits at high-T to the lattice heat capacity help us fix $\beta = 3 \times 10^{-4}\ \text{J/mol K}^4$ (see SM [28]). As the lattice contribution in the low-T range is negligible, we get very similar parameter values $\gamma_{\text{avg}} = 16\ \text{mJ/mol K}^2$, $\alpha_{\text{avg}} = 15\ \text{mJ/mol K}^3$ with $f = 2.5\%$. Most importantly, the fitting significantly worsens *without* a T^2 component and can not be considered as fitting the data (see SM [28]).

As far as $S = \frac{1}{2}$ triangular lattice spin liquids are concerned, a linear variation of the low-temperature specific heat was observed in κ-$(BEDT\text{-}TTF)_2Cu_2(CN)_3$ [18] and $Ba_3CuSb_2O_9$ [22]. This was interpreted in terms of a spinon Fermi surface. However, the T^2 term in $C_m(T)$ observed at low-T in SCSO is perhaps the first such observation in triangular $S = \frac{1}{2}$ magnets. From this crucial presence of T^2 contributions, we infer the presence of gapless excitations with a linear dispersion [42]. Within a Dirac QSL phenomenology that naturally gives such excitations, we can estimate the magnetic exchange strength from low-temperature specific heat data to compare with previous estimates from high-temperature data. We take the following effective mean-field Hamiltonian as our Dirac QSL ansatz $\mathcal{H} = (J_{\text{eff}}/2)\sum_{\langle i,j\rangle \in \triangle\text{lattice},\sigma} \chi_{ij} c^{\dagger}_{i,\sigma} c_{j,\sigma} + \text{H.c.}$ such that π flux is inserted in the up triangles [13,44]. J_{eff} is expected to be the same order as the dominant exchange [$J_{\text{eff}} \sim \mathcal{O}(J_1)$] Near the single Dirac cone in

the Brillouin zone (see SM [28] for details), the effective low-energy spectrum is $\epsilon_{\mathbf{k}} = \pm\sqrt{3/2}J_{\text{eff}}k$. Therefore at low temperatures ($T \to 0$), we obtain $[C(T)/k_B] = 2.292[(k_BT)^2/J_{\text{eff}}^2]$. In the presence of Zeeman coupling to an external magnetic field, this gets modified to $[C(T)/k_B] \approx 2.292[(k_BT)^2/J_{\text{eff}}^2] + 0.696\{[(k_BT)(g\mu_B|H|/2)]/J_{\text{eff}}^2\}$ as $(g\mu_B|H|/2k_BT) \gg 1$, which is indeed the functional form used earlier for fits. From the coefficient α_{avg} of the T^2 contribution, we estimate $(J_1/k_B) \sim 36$ K. This completely independent low-T, macroscopic, or thermodynamic estimate for J_1 is of the same order as the previous estimate from high-T susceptibility data which we consider to be significant [45]. In fact, from the low-field values of α, the estimate is $(J_1/k_B) \sim 76$ K. Furthermore, these estimates also agree with microscopic estimates based on a DFT study of the SCSO perovskite system to be discussed soon.

We finally note an anomaly that is present in the heat capacity data at low fields, seen as a "separation" between the curves as we go from 10 to 30 kOe in Fig. 5. This is also reflected in the fits based on our linearly dispersing Dirac QSL ansatz as a jump in α and γ at these fields as seen in the inset of Fig. 5. Note that the Schottky gap is nonzero even in the absence of a magnetic field for SCSO (see SM [28]) which is a feature seen in other QSLs as well [22,40,41] and is ascribed to interaction of the orphan spins with the correlated regions. We speculate this happens when the orphan spins suddenly decouple from the correlated regions as the applied field exceeds ~10 kOe (which might be the effective internal field strength of their interaction). Since this "separation" in the data sets at low field is observed in the raw or as-measured C_p data prior to any fitting, we think that it has a distinct physical origin (leading to an artificial jump in α, γ parameters when using a fitting form based on assuming only linear-dispersing excitations). There could be other explanations for this observation as well. Also for $H \geq 30$ kOe, a slight decrease of γ with field is found from the data whereas an increase is predicted by our ansatz, while α remains roughly independent of field as predicted by our ansatz. Nonetheless, another supporting feature in the data is that the ratio of the quadratic and linear components agrees with the theoretical value quite well for $H = 50$ kOe and to within a factor of 3 for all $H \geq 30$ kOe data sets despite the anomalous field dependence of γ. The deviations suggest that something else may also be contributing to the heat capacity in addition to the linearly dispersing excitations. We remark here that (1) $(g\mu_B|H|/2k_BT) \gg 1$ is not strictly true for the applied fields, and (2) that our ansatz is at a mean-field level, though the T^2 behavior is robust to beyond mean-field effects for a Dirac QSL [46,47].

To check the viability of a Dirac QSL phenomenology argued above as arising from a triangular quantum magnet with further-neighbor frustrating antiferromagnetic exchanges [11–13], we have carried out first principles electronic structure calculations based on DFT for the experimentally determined triple perovskite structure of $Sr_3CuSb_2O_9$. All the electronic structure calculations are carried out using DFT in the pseudopotential plane-wave basis within the generalized gradient approximation [48] supplemented with Hubbard U [49] as encoded in the Vienna *ab initio* simulation package (VASP) [50,51] with projector augmented wave potentials [52,53]. The calculations are done with standard values of $U_{\text{eff}} \equiv U_d - J_H = 6.5$ eV [49] chosen for Cu. The non-spin-polarized total and Cu d partial density of states (DOS) for SCSO (see SM [28]) reveal that the Fermi level is dominated by partially filled Cu e_g states. The oxygen O p states are completely occupied while Sb s and p states and Sr s states are completely empty consistent with the nominal ionic formula, $Sr_3^{2+}Cu^{2+}Sb_2^{5+}O_9^{2+}$ of this compound. Spin polarized calculations with ferromagnetic arrangement of Cu spins yields total moment 1.0 μ_B per formula unit, which further supports the $S = \frac{1}{2}$ moment of Cu and is consistent with the experimentally determined effective moment ($\mu_{\text{eff}} = 1.72\ \mu_B$). However, the calculated magnetic moment per Cu site is 0.80 μ_B, while the rest of the moment is hosted on the ligand sites due to substantial hybridization of Cu with ligands.

To estimate the exchange interactions, we consider the following Hamiltonian $H = J_1 \sum_{\langle i,j\rangle}^{\text{intra}} \mathbf{S}_i.\mathbf{S}_j + J_2 \sum_{\langle\langle i,j\rangle\rangle}^{\text{intra}} \mathbf{S}_i \cdot \mathbf{S}_j + J_1^{\perp} \sum_{\langle i,j\rangle}^{\text{inter}} \mathbf{S}_i \cdot \mathbf{S}_j + J_2^{\perp} \sum_{\langle i,j\rangle}^{\text{inter}} \mathbf{S}_i \cdot \mathbf{S}_j$. Here, J_1, J_2, $J_1^{\perp}$, and $J_2^{\perp}$ are, respectively, the nearest-neighbor, the next-nearest-neighbor intralayer and (two distinct) interlayer Heisenberg exchange parameters. We have calculated them employing the "four state" method [54,55]. This is based on a computation of the total energy of the system with collinear spin alignment, where the spin configuration on two chosen sites are modified while restricting rest of the spins to a base configuration. Our calculations reveal that the estimates of the exchange interactions change up to 15% depending on the chosen base configuration. We find $J_1 \sim 3.92$ meV ($J_1/k_B \sim 45$ K) to be the dominant antiferromagnetic exchange in this system. This microscopic estimate agrees well with the values extracted from the high-temperature susceptibility data and low-temperature specific heat data. $J_1^{\perp} \sim 0.21$ meV and $J_2^{\perp} \sim 0.11$ meV are found to be subdominant and robustly antiferromagnetic, thus adding to the frustration. $J_2 \sim 0.05$ meV was even smaller, and its sign also depended on the chosen base configuration. This last estimate is at the edge of the accuracy of our DFT calculations (~0.05 meV). The strength of the further-neighbor exchanges are relatively much smaller because the Cu atoms are far apart, as well as the intermediate Sb atoms are smaller in size. Our first principles DFT results corroborates well with the experimental results, and lends credence to the scenario of spin liquid behavior induced by further-neighbor frustrating exchanges [11–13].

Summary.—Our comprehensive set of data on SCSO show a 1:2 site ordering between Cu and Sb ions (giving rise to nearly isolated $S = \frac{1}{2}$ triangular planes) and a lack of LRO together with the presence of dynamic moments down to the lowest temperatures (65 mK, which is well below $\theta_{CW} = -143$ K). In contrast to other kagome or pyrochlore based QSL, here the magnetic heat capacity at low T follows $C_m = \gamma T + \alpha T^2$. The T^2 behavior of C_m evinces the presence of gapless excitations with a linear dispersion, and the dominant exchange extracted through such a phenomenology agrees quantitatively with those from high-temperature susceptibility data and DFT estimates. We believe that the presence of further-neighbor antiferromagnetic exchanges induces Dirac QSL behavior in the triangular lattice system of SCSO. Our work offers new material directions to explore in the field of QSLs. Further work to unravel the magnitude of the further-neighbor couplings or possibly ring exchange terms [56,57] in promoting the spin liquid state is clearly warranted.

We thank MHRD and Department of Science and Technology, Government of India for financial support. We also thank Nandini Trivedi and Subhro Bhattacharjee for useful discussion and late Christoph Klausnitzer for technical support. Experiments at the ISIS Neutron and Muon Source were supported by a beam-time allocation RB1910129 from the Science and Technology Facilities Council. S. P. acknowledges financial support from Industrial Research and Consultancy Centre, IIT Bombay (17IRCCSG011) and SERB, DST, India (SRG/2019/001419). I. D. G. acknowledges financial support from Technical Research Centre DST and SERB India. A. V. M., I. D. G., and S. P. acknowledge hospitality and support of ICTS and APCTP during the second Asia Pacific Workshop on Quantum Magnetism (Code:ICTS/apfm2018/11).

*skundu37@gmail.com
†mahajan@phy.iitb.ac.in

[1] P. Fazekas and P. W. Anderson, Philos. Mag. **30**, 423 (1974).
[2] Y. Zhou, K. Kanoda, and T.-K. Ng, Rev. Mod. Phys. **89**, 025003 (2017).
[3] H. Kadowaki, H. Takei, and K. Motoya, J. Phys. Condens. Matter **7**, 6869 (1995).
[4] R. Ishii, S. Tanaka, K. Onuma, Y. Nambu, M. Tokunaga, T. Sakakibara, N. Kawashima, Y. Maeno, C. Broholm, D. P. Gautreaux, J. Y. Chan, and S. Nakatsuji, Europhys. Lett. **94**, 17001 (2011).
[5] Y. Shirata, H. Tanaka, A. Matsuo, and K. Kindo, Phys. Rev. Lett. **108**, 057205 (2012).
[6] D. A. Huse and V. Elser, Phys. Rev. Lett. **60**, 2531 (1988).
[7] T. Jolicoeur and J. C. Le Guillou, Phys. Rev. B **40**, 2727 (1989).
[8] R. R. P. Singh and D. A. Huse, Phys. Rev. Lett. **68**, 1766 (1992).
[9] B. Bernu, P. Lecheminant, C. Lhuillier, and L. Pierre, Phys. Rev. B **50**, 10048 (1994).
[10] L. Capriotti, A. E. Trumper, and S. Sorella, Phys. Rev. Lett. **82**, 3899 (1999).
[11] R. Kaneko, S. Morita, and M. Imada, J. Phys. Soc. Jpn. **83**, 093707 (2014).
[12] Z. Zhu and S. R. White, Phys. Rev. B **92**, 041105(R) (2015).
[13] Y. Iqbal, W.-J. Hu, R. Thomale, D. Poilblanc, and F. Becca, Phys. Rev. B **93**, 144411 (2016).
[14] J. Knolle and R. Moessner, Annu. Rev. Condens. Matter Phys. **10**, 451 (2019).
[15] Y. Shimizu, K. Miyagawa, K. Kanoda, M. Maesato, and G. Saito, Phys. Rev. Lett. **91**, 107001 (2003).
[16] T. Itou, A. Oyamada, S. Maegawa, Z. Tamura, and R. Kato, J. Phys. Condens. Matter **19**, 145247 (2007).
[17] T. Itou, A. Oyamada, S. Maegawa, M. Tamura, and R. Kato, Phys. Rev. B **77**, 104413 (2008).
[18] S. Yamashita, Y. Nakazawa, M. Oguni, Y. Oshima, H. Nojiri, Y. Shimizu, K. Miyagawa, and K. Kanoda, Nat. Phys. **4**, 459 (2008).
[19] J. A. Paddison, M. Daum, Z. Dun, G. Ehlers, Y. Liu, M. Stone, H. Zhou, and M. Mourigal, Nat. Phys. **13**, 117 (2017).
[20] M. Baenitz, P. Schlender, J. Sichelschmidt, Y. A. Onykiienko, Z. Zangeneh, K. M. Ranjith, R. Sarkar, L. Hozoi, H. C. Walker, J.-C. Orain, H. Yasuoka, J. van den Brink, H. H. Klauss, D. S. Inosov, and T. Doert, Phys. Rev. B **98**, 220409(R) (2018).
[21] R. Sarkar, P. Schlender, V. Grinenko, E. Haeussler, P. J. Baker, T. Doert, and H.-H. Klauss, Phys. Rev. B **100**, 241116(R) (2019).
[22] H. D. Zhou, E. S. Choi, G. Li, L. Balicas, C. R. Wiebe, Y. Qiu, J. R. D. Copley, and J. S. Gardner, Phys. Rev. Lett. **106**, 147204 (2011).
[23] Y. Ishiguro, K. Kimura, S. Nakatsuji, S. Tsutsui, A. Q. R. Baron, T. Kimura, and Y. Wakabayashi, Nat. Commun. **4**, 2022 (2013).
[24] A. A. Bush and V. P. Sirotinkin, Inorg. Mater. **44**, 1233 (2008).
[25] D. C. Wallace and T. M. McQueen, Dalton Trans. **44**, 20344 (2015).
[26] J. T. Rijssenbeek, S. Malo, V. Caignaert, and K. R. Poeppelmeier, J. Am. Chem. Soc. **124**, 2090 (2002).
[27] J. R. Carvajal, in *Proceedings of the Satellite Meeting on Powder Diffraction of the XV Congress of the IUCr*, 1990 (unpublished); see also at https://www.ill.eu/sites/fullprof/index.html.
[28] See Supplemental Material at http://link.aps.org/supplemental/10.1103/PhysRevLett.125.267202 for details, which includes Refs. [29–32].
[29] K. Momma and F. Izumi, J. Appl. Crystallogr. **44**, 1272 (2011).
[30] Y. Han, M. Hagiwara, T. Nakano, Y. Nozue, K. Kimura, M. Halim, and S. Nakatsuji, Phys. Rev. B **92**, 180410(R) (2015).
[31] K. Y. Zeng, L. Ma, Y. X. Gao, Z. M. Tian, L. S. Ling, and L. Pi, Phys. Rev. B **102**, 045149 (2020).
[32] X.-G. Wen, *Quantum Field Theory of Many-Body Systems: From the Origin of Sound to an Origin of Light and Electrons* (Oxford University Press, Oxford, 2007).

[33] N. Elstner, R. R. P. Singh, and A. P. Young, Phys. Rev. Lett. **71**, 1629 (1993).
[34] M. Tamura and R. Kato, J. Phys. Condens. Matter **14**, L729 (2002).
[35] Y. Haraguchi, C. Michioka, M. Imai, H. Ueda, and K. Yoshimura, Phys. Rev. B **92**, 014409 (2015).
[36] Subdominant exchange couplings are assumed to not affect the susceptibility significantly in the high-temperature regime which is primarily controlled by the dominant exchange coupling.
[37] A CW fit at high-T, yields $\chi_0 = -1.61 \times 10^{-4}$ cm^3/mol Cu, $C = 0.384$ K cm^3/mol Cu, and the $\theta_{\rm CW} = -143$ K. The inferred effective moment $\mu_{\rm eff} = 1.75\ \mu_B$ is close to the expected value of $1.73\ \mu_B$ for S $= 1/2$ Cu^{2+} ion with $g = 2$. A negative $\theta_{\rm CW}$ indicates antiferromagnetic correlations between the Cu^{2+} ions.
[38] Similar conclusions were drawn from our electron spin resonance (ESR) and nuclear magnetic resonance (NMR) experiments (see SM [28]).
[39] Y. Li, D. Adroja, P. K. Biswas, P. J. Baker, Q. Zhang, J. Liu, A. A. Tsirlin, P. Gegenwart, and Q. Zhang, Phys. Rev. Lett. **117**, 097201 (2016).
[40] M. A. de Vries, K. V. Kamenev, W. A. Kockelmann, J. Sanchez-Benitez, and A. Harrison, Phys. Rev. Lett. **100**, 157205 (2008).
[41] T.-H. Han, R. Chisnell, C. J. Bonnoit, D. E. Freedman, V. S. Zapf, N. Harrison, D. G. Nocera, Y. Takano, and Y. S. Lee, http://arxiv.org/abs/1402.2693v1.
[42] A quadratic temperature dependence of the magnetic specific heat was seen in high-pressure prepared cubic phase of $S = 1$ $Ba_3NiSb_2O_9$ [43]. This observation was completely field independent unlike our $S = \frac{1}{2}$ observations. Such field-independent quadratic dependence is thought to arise from quadrupolar ordering in pristine $S = 1$ triangular systems, however, the triangular planes are diluted in the compound $Ba_3NiSb_2O_9$.
[43] J. G. Cheng, G. Li, L. Balicas, J. S. Zhou, J. B. Goodenough, C. Xu, and H. D. Zhou, Phys. Rev. Lett. **107**, 197204 (2011).
[44] Y.-M. Lu, Phys. Rev. B **93**, 165113 (2016).
[45] This estimate for the scale of J_1 is in the high-temperature side of the specific heat data, thus the approximations of using the low-energy form of the spectrum and $T \to 0$ are justified *a posteriori*.
[46] Y. Ran, M. Hermele, P. A. Lee, and X.-G. Wen, Phys. Rev. Lett. **98**, 117205 (2007).
[47] D. H. Kim, P. A. Lee, and X.-G. Wen, Phys. Rev. Lett. **79**, 2109 (1997).
[48] J. P. Perdew, K. Burke, and M. Ernzerhof, Phys. Rev. Lett. **77**, 3865 (1996).
[49] V. I. Anisimov, J. Zaanen, and O. K. Andersen, Phys. Rev. B **44**, 943 (1991).
[50] G. Kresse and J. Hafner, Phys. Rev. B **47**, 558 (1993).
[51] G. Kresse and J. Furthmüller, Phys. Rev. B **54**, 11169 (1996).
[52] P. E. Blöchl, Phys. Rev. B **50**, 17953 (1994).
[53] G. Kresse and D. Joubert, Phys. Rev. B **59**, 1758 (1999).
[54] H. J. Xiang, E. J. Kan, S.-H. Wei, M.-H. Whangbo, and X. G. Gong, Phys. Rev. B **84**, 224429 (2011).
[55] R. Kumar, T. Dey, P. M. Ette, K. Ramesha, A. Chakraborty, I. Dasgupta, R. Eremina, S. Tóth, A. Shahee, S. Kundu, M. Prinz-Zwick, A. A. Gippius, H. A. K. von Nidda, N. Büttgen, P. Gegenwart, and A. V. Mahajan, Phys. Rev. B **99**, 144429 (2019).
[56] O. I. Motrunich, Phys. Rev. B **72**, 045105 (2005).
[57] T. Grover, N. Trivedi, T. Senthil, and P. A. Lee, Phys. Rev. B **81**, 245121 (2010).